Energy Fuels **2010,** *24,* 1617–1627 · DOI:10.1021/ef901292j
Published on Web 02/26/2010

energy&fuels
article

Methane/*n*-Butane Ignition Delay Measurements at High Pressure and Detailed Chemical Kinetic Simulations

D. Healy,[†] M. M. Kopp,[‡] N. L. Polley,[‡] E. L. Petersen,[‡] G. Bourque,[§] and H. J. Curran*[,†]

[†]*Combustion Chemistry Centre, School of Chemistry, National University of Ireland (NUI) Galway, University Road, Galway, Ireland,* [‡]*Department of Mechanical Engineering, Texas A&M University, College Station, Texas 77843, and* [§]*Rolls-Royce Canada Limited, 9500 Côte de Liesse, Lachine, Québec H8T 1A2, Canada*

Received November 3, 2009. Revised Manuscript Received February 4, 2010

Autoignition delay time measurements were recorded for blends of $CH_4/n\text{-}C_4H_{10}$ in "air" at pressures of approximately 10, 16, 20, 25, and 30 atm from fuel-lean to fuel-rich conditions at two different fuel compositions, 90% CH_4/10% $n\text{-}C_4H_{10}$ and 70% CH_4/30% $n\text{-}C_4H_{10}$, and temperatures from 660 to 1330 K in both a rapid compression machine and a shock-tube facility. A detailed chemical kinetic model consisting of 1328 reactions involving 230 species was validated using the ignition delay data from this study. This mechanism has already been used to simulate previously published ignition delay times over a wide range of conditions. It was found that the model quantitatively reproduces the ignition delays from both rapid compression and reflected shock waves, accurately capturing reactivity as a function of the temperature, pressure, equivalence ratio, and fuel composition.

1. Introduction

Successful operation of a gas turbine requires, first, that ignition occurs and, second, that it occurs only in the combustor. Ignition can sometimes take place prior to the mixed fuel and air reaching the combustor zone; i.e., if premature ignition takes place in the premix duct prior to the combustion chamber, potential damage to the premixing hardware could occur, with the associated loss of emissions performance.

The fuel flexibility of gas turbines is also of great importance to the gas turbine industry, because reactivity is dependent upon composition, which is known to vary from one gas field to another. Turbines are operated on not only natural gas but also lignite coal and other carbonaceous fuels, making the study of natural gas blends at extremes of composition, such as those in the current study, of particular importance because they offer a more realistic parallel to the real composition of the broad range of gas turbine fuels than either their single-component or non-extreme binary counterparts. Fundamental measurements of the ignition delay times of blends of methane seeded with *n*-butane at pressures and concentrations analogous to those of gas turbines have been carried out in both rapid compression machine (RCM) and shock-tube facilities.

Although the fractional contribution of both butane isomers to the composition of conventional natural gas is small, the contribution of either butane isomer cannot be ignored when considering the combustion chemistry of natural gas surrogates. The work in this paper is designed to amplify the work of three previous publications concerning the autoignition of the butane isomers.[1−3] The primary concern of the current study is to investigate the autoignition of binary mixtures of $CH_4/n\text{-}C_4H_{10}$ at 90/10% and 70/30% in the low- to intermediate-temperature region at varying pressures and equivalence ratios. We aim to extend the limited studies that have already been carried out on the autoignition of binary mixtures of $CH_4/n\text{-}C_4H_{10}$ to further the understanding of the combustion chemistry of the butanes, particularly at low temperatures, because most previous studies were centered around the high-temperature and low-pressure combustion of blends with lower $n\text{-}C_4H_{10}$ content than the current study.

For example, Higgin and Williams[4] conducted ignition delay time studies of shock-heated $CH_4/n\text{-}C_4H_{10}$ mixtures in the temperature range of 1800−2500 K at $\phi = 0.5$. Using 90% argon as the diluent and approximately 8% O_2, the $n\text{-}C_4H_{10}$ fuel fraction was varied between 1, 3.7, and 12.5%. The authors found that, upon increasing the $n\text{-}C_4H_{10}$ contribution from 1 to 3.7%, the ignition delay time was reduced by a factor of 6, while increasing the $n\text{-}C_4H_{10}$ concentration to 12.5% reduced the ignition delay time by an order of magnitude. However, the data from their study have a limited value for comparison to other data because only an initial pressure range of 0.26−0.39 atm was quoted for the entire set of experiments, with no clarification of the conditions of any individual experiment.

Burcat et al.[5] and Zellner et al.[6] carried out a systematic investigation of the ignition delay times of the alkanes from CH_4 to C_5H_{12} and their methane-based binary mixtures. The study, although containing valuable ignition delay data for many hydrocarbons and their blends, only concerns itself

*To whom correspondence should be addressed: Combustion Chemistry Centre, School of Chemistry, NUI Galway, University Road, Galway, Ireland. Telephone: 00353-91-493856. E-mail: henry.curran@nuigalway.ie. Website: http://c3.nuigalway.ie/.

(1) Healy, D.; Donato, N. S.; Aul, C. J.; Petersen, E. L.; Zinner, C. M.; Bourque, G.; Curran, H. J. *Combust. Flame* **2010**, http://dx.doi.org/10.1016/j.combustflame.2010.01.016.

(2) Healy, D.; Donato, N. S.; Aul, C. J.; Petersen, E. L.; Zinner, C. M.; Bourque, G.; Curran, H. J. *Combust. Flame* **2010**, http://dx.doi.org/10.1016/j.combustflame.2010.01.011.

(3) Donato, N.; Aul, C.; Petersen, E.; Zinner, C.; Healy, D.; Curran, H.; Bourque, G. *J. Eng. Gas Turbines Power* **2010**, in press.

(4) Higgin, R. M. R.; Williams, A. *Proc. Combust. Inst.* **1969**, *12*, 579.

(5) Burcat, A.; Scheller, K.; Lifshitz, A. *Combust. Flame* **1971**, *16*, 29.

(6) Zellner, R.; Niemitz, K. J.; Warnatz, J.; Gardiner, W. C., Jr.; Eubank, C. S.; Simmie, J. M. *Prog. Aeronaut. Astronaut.* **1983**, *88*, 252.

Table 1. $CH_4/n\text{-}C_4H_{10}$ Mixtures Tested

mix	percentage of CH_4	percentage of $n\text{-}C_4H_{10}$	percentage of O_2	percentage of diluent	ϕ	P(atm)	T(K)
90/10	0.024	0.003	0.204	0.769	0.32	10, 20, 30	780−1080
90/10	0.039	0.004	0.201	0.756	0.53	10, 16, 20, 26, 30	770−1340
90/10	0.075	0.008	0.192	0.724	1.07	10, 16, 20, 26, 30	720−1050
90/10	0.139	0.015	0.178	0.668	2.13	20, 30	700−940
70/30	0.015	0.006	0.206	0.773	0.35	20, 30	700−960
70/30	0.024	0.010	0.203	0.762	0.58	10, 20, 30	700−1065
70/30	0.047	0.020	0.196	0.737	1.16	10, 20, 30	680−970
70/30	0.089	0.038	0.183	0.690	2.31	10, 20, 30	680−830

with $CH_4/iso\text{-}C_4H_{10}$ mixtures in the temperature range of 1250−1900 K and not $CH_4/n\text{-}C_4H_{10}$.

Crossley et al.[7] studied the effect of butane addition to methane by measuring ignition delay times behind reflected shock waves at pressures between 7 and 11 atm in the temperature range of 1370−1870 K. In these experiments, the initial charge density for both blends was also maintained at 0.21 atm, leading to an increase in the test temperature as the temperature of the experiment is increased. Using argon as the diluent, the CH_4 and O_2 fractions of the blends studied were held constant at 3.5 and 7%, respectively, and the $n\text{-}C_4H_{10}$ contribution was varied from 0.05 to 0.155%. The data of Crossley et al. also showed the same trend as those of Higgin and Williams; i.e., the addition of $n\text{-}C_4H_{10}$ accelerated the oxidation of methane over the temperature range studied.

Spadaccini and Colket[8] in a study similar to that of Crossely et al. using argon as the diluent also investigated ignition delay times for $CH_4/n\text{-}C_4H_{10}$ blends behind reflected shock waves at 1300−1700 K and pressures between 5.5 and 9 atm. For these experiments, the O_2 fraction was maintained at 7% and the $CH_4/n\text{-}C_4H_{10}$ fractions were varied to give two binary mixtures of 3.4% CH_4/0.1%$n\text{-}C_4H_{10}$ and 3.3% CH_4/0.21% $n\text{-}C_4H_{10}$. Spadaccini and Colket studied the effect of blending C_4H_{10} with C_2H_6 and C_3H_8 and found that the butanes were more effective in reducing ignition delay than either C_2H_6 or C_3H_8, but there was little difference found between *n*- and $iso\text{-}C_4H_{10}$ over the range of conditions studied.

de Vries and Petersen[9] studied the autoignition of blends of CH_4/C_4H_{10}, $CH_4/C_2H_6/C_4H_{10}$, $CH_4/C_2H_6/C_3H_8/C_4H_{10}$, and $CH_4/C_4H_{10}/C_5H_{12}$ behind reflected shock waves at high pressure (ca. 20 atm) and temperature near 800 K. In this work, de Vries and Petersen reported that there was little difference between the addition of 25 and 50% of C_2-C_5 hydrocarbons to the oxidation of CH_4 at these conditions. Unfortunately, their experiments were performed at very low temperatures and higher pressures, and the resulting shock-tube data exhibited early reactivity and dramatic pressure rises that led to an acceleration of the main ignition event.

Finally, Gersen et al.[10] studied $CH_4/n\text{-}C_4H_{10}$, $CH_4/iso\text{-}C_4H_{10}$, and $iso\text{-}C_4H_{10}/n\text{-}C_4H_{10}$ autoignition in a RCM at intermediate temperatures (890−1100 K) between 15 and 45 atm. Gersen et al. presented ignition delays for binary blends of 97% CH_4 and 3% C_4H_{10} at two equivalence ratios, $\phi = 0.5$ and 1.0. In the temperature range studied, the authors did not see a marked difference between the promoting effects of either butane isomer on pure methane.

(7) Crossley, R. W.; Dorko, E. A.; Scheller, K.; Burcat, A. *Combust. Flame* **1972**, *19*, 373.
(8) Spadaccini, L. J.; Colket, M. B., III. *Prog. Energy Combust. Sci.* **1994**, *20* (5), 431.
(9) de Vries, J.; Petersen, E. L. *Proc. Combust. Inst.* **2007**, *31*, 3163.
(10) Gersen, S.; Mokhov, A. V.; Levinsky, H. B. European Combustion Meeting, Vienna, Austria, 2009; ECM Paper 810293.

2. Experimental Section

Details of both the RCM[11−13] and the shock tubes[14−16] have been provided previously but are discussed briefly in this section. Table 1 provides details of the mixtures used in the study. Provided first is a summary of the RCM facility, followed by a summary of the shock tubes.

2.1. RCM. Briefly, the NUI Galway RCM (previously the Shell−Thornton RCM[17]) comprises a twin opposed piston configuration. This twin piston design results in a fast compression time of a little over 16 ms; thus, the NUI Galway RCM experiences significantly less heat loss during the compression sequence than many other RCMs, although they do still occur. Creviced pistons were used to increase postcompression temperature homogeneity. Experiments were carried out at a compression ratio close to 10, although as discussed previously,[18] the effective compression ratio was found to be lower when pure argon was used as the diluent and higher when pure nitrogen was used. To vary the compressed-gas temperature, T_C, two approaches were used: (i) the proportions of diluent gases (N_2/Ar) were varied to vary the overall heat capacity of the fuel and "air" mixture, and (ii) an electrothermal, digitally controlled heating system surrounds the combustion chamber allowing for the initial temperature to be varied from ambient to a maximum operating temperature of 393 K. Both the heating system and combustion chamber are insulated to maximize the temperature control.

Methane and *n*-butane gases were obtained from Aldrich at 99%+ purity, while all other gases were supplied by BOC Ireland; 99.95% nitrogen (CP grade), 99.9995% argon (research grade), and 99.5% oxygen (medical grade) were all used without further purification. Test mixtures were prepared manometrically in a stainless-steel container and allowed to mix overnight before use.

Pressure−time data were measured using a Kistler 603B pressure transducer in conjunction with a Kistler 5007 amplifier and relayed to a Nicolet Sigma 90-4 oscilloscope, where they were then recorded at a resolution of 1 megasample/s. Chamber windows were replaced with aluminum blanks to reinforce the integrity; this was necessary because the maximum tolerance of the chamber was breached on several occasions upon ignition. The ignition delay time, defined as the time from the end of compression to the maximum rate of pressure rise during ignition, is measured using two vertical cursors on the oscilloscope. In general, ignition delay times were reproducible to

(11) Brett, L. Ph.D. Thesis, National University of Ireland, Galway, Ireland, 1999.
(12) Brett, L.; MacNamara, J.; Musch, P.; Simmie, J. M. *Combust. Flame* **2001**, *124*, 326.
(13) Gallagher, S.; Curran, H. J.; Metcalfe, W. K.; Healy, D.; Simmie, J. M.; Bourque, G. *Combust. Flame* **2007**, *153*, 316.
(14) Petersen, E. L.; Kalitan, D. M.; Simmons, S.; Bourque, G.; Curran, H. J.; Simmie, J. M. *Proc. Combust. Inst.* **2007**, *31*, 447.
(15) Petersen, E. L.; Rickard, M. J. A.; Crofton, M. W.; Abbey, E. D.; Traum, M. J.; Kalitan, D. M. *Meas. Sci. Technol.* **2005**, *16*, 1716.
(16) Aul, C. J. Masters Thesis, Texas A&M University, College Station, TX, 2009.
(17) Affleck, W. S.; Thomas, A. *Proc. Inst. Mech. Eng.* **1968−1969**, *183* (1), 365.
(18) Healy, D.; Curran, H. J.; Simmie, J. M.; Kalitan, D. M.; Petersen, E. L.; Bourque, G. *Combust. Flame* **2008**, *155*, 451.

within 10% of one another at each T_C. The compressed gas pressure was measured using two horizontal cursors. The gas mixtures together with the initial conditions and experimental ignition delay time results are documented in the Supporting Information. It should be noted that, for these experiments, which used 90/10% and 70/30% methane/*n*-butane as fuel, we did not observe any two-stage ignition events involving cool flames, even though there is a pronounced NTC behavior observed for the 70% methane/30% *n*-butane mixtures, and that *n*-butane does display pronounced two-stage ignition behavior.[19−26] The compressed gas temperature, T_C, was calculated using the initial temperature, T_i, pressure, p_i, the reactant composition, and the experimentally measured compressed gas pressure, p_C, defined as the maximum pressure immediately after compression, and employing the adiabatic compression/expansion routine in Gaseq,[27] which uses the temperature dependence of the ratio of specific heats, γ, according to the equation

$$\ln\left(\frac{p_C}{p_i}\right) = \int_{T_i}^{T_C} \frac{\gamma}{\gamma - 1}\frac{dT}{T}$$

assuming frozen chemistry during compression.

2.2. Shock Tube. Each of the methane/*n*-butane mixtures was tested behind reflected shock waves using two shock-tube facilities, both of which are capable of test pressures up to 100 atm and test temperatures up to 5000 K. One facility consists of a 10.7 m driven section having a circular cross-section with an internal diameter of 16.2 cm and a 3.5 m driver section having a circular cross-section with a 7.62 cm internal diameter. The second shock-tube facility contains a 4.72 m driven section with a 15.24 cm internal diameter and a 4.92 m driver section with a 7.62 cm inner diameter. Both shock tubes are made of stainless-steel 304 and are described in greater detail by Petersen et al.[15] and Aul.[16]

In both shock tubes, helium is used as the driver gas, which is separated from the driven section by either an aluminum or a polycarbonate diaphragm, depending upon the desired test pressure. The methane/*n*-butane/air blends were made of ultra-high-purity gases and were mixed using partial pressures in a separate mixing tank. The air was a mixture of 99.9995% purity N_2 and O_2 at a molar ratio of 3.76:1. The *n*-butane had a purity level of 99.95%.

Test temperatures and pressures were determined by measuring the incident-shock velocity and using the one-dimensional shock relations. Five pressure transducers, mounted in series along the shock tube, send signals to four timer counter boxes (Fluke PM 6666), which are then used to extrapolate the incident-shock velocity to its value at the end wall. Ignition delay times are measured from the sharp increase in the endwall pressure trace, which occurs behind the reflected shock wave. The onset of OH* emission should coincide with this sharp rise in pressure, as shown in Figure 1 from ports located at the endwall of the shock tube. Piezoelectric pressure transducers monitor the pressure from both an endwall and a sidewall location, while photomultiplier tubes monitor the OH* emission through a 10 nm wide narrowband filter centered at 310 nm at both locations as well.

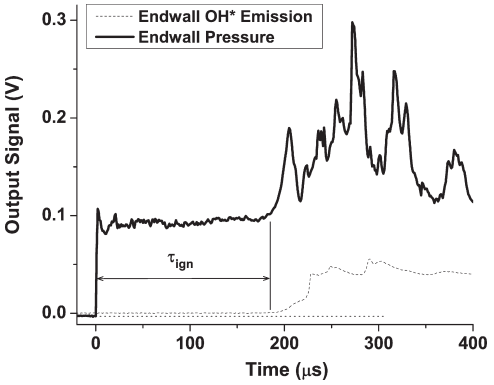

Figure 1. Example endwall pressure and OH* emission traces used to determine ignition delay time for 70/30% methane/*n*-butane blend and $\phi = 2.31$, at 1273 K and 18.5 atm.

3. Computational Kinetic Mechanism

A chemical kinetic mechanism was developed, and simulations were performed using the hydrodynamics, chemistry, and transport (HCT) program.[28] The detailed chemical kinetic mechanism is based on the hierarchical nature of hydrocarbon combustion mechanisms containing the H_2/O_2 submechanism,[29] together with the CO/CH_4 and the C_2 and C_3 submechanisms that have already been published.[14,18,30] The C_4 submechanism has been fully detailed in two recent papers on the butane isomers.[1,2] The version of the model used in the current work is C5_49, which is available online together with associated thermochemical parameters at http://c3.nuigalway.ie/mechanisms.html.

4. Results and Discussion

4.1. Simulation. Heat losses need to be considered when simulating RCM experiments because of the magnitude of the ignition delay time; in this study alone, the range of ignition delay times is between 3 and 259 ms. A delay time of 259 ms allows for a significant amount of time for substantial heat losses to occur. Therefore, it is necessary to quantify heat loss to realistically simulate an RCM experiment. To this end, a series of nonreactive experiments was performed, in which the O_2 content of the mixture was replaced with N_2. These experiments were then simulated, and heat-loss coefficients in the form of zone/piston velocities were recorded for each condition. This type of simulation has been described by us previously[13] but is briefly discussed again here. Figures 2−6 in the Supporting Information show the comparison of the simulation and measurement for nonreactive pressure traces. Essentially, we treat each experiment as an adiabatic compression followed by an adiabatic expansion to account for heat losses. This type of

(19) Franck, J.; Griffiths, J. F.; Nimmo, W. *Proc. Combust. Inst.* **1986**, *21*, 447.
(20) Carlier, M.; Corre, C.; Minetti, R.; Pauwels, J. F.; Ribaucour, M.; Sochet, L. R. *Proc. Combust. Inst.* **1990**, *23*, 1753.
(21) Minetti, R.; Ribaucour, M.; Carlier, M.; Fittschen, C.; Sochet, L. R. *Combust. Flame* **1994**, *96*, 201.
(22) Minetti, R.; Ribaucour, M.; Carlier, M.; Sochet, L. R. *Combust. Sci. Technol.* **1996**, *113−114*, 179.
(23) Kojima, S.; Suzuoki, T. *Combust. Flame* **1993**, *92* (3), 254.
(24) Griffiths, J. F.; Halford-Maw, P. A.; Rose, D. J. *Combust. Flame* **1993**, *95*, 291.
(25) Gersen, S.; Mokhov, A. V.; Darmeveil, J. H.; Levinsky, H. B. *Combust. Flame* **2010**, *157*, 240.
(26) Healy, D.; Donato, N. S.; Aul, C. J.; Petersen, E. L.; Zinner, C. M.; Bourque, G.; Curran, H. J. *Combust. Flame* **2010**, in press.
(27) Morley, C. http://www.arcl02.dsl.pipex.com/gseqrite.htm.
(28) Lund, C. M.; Chase, L. HCT—A general computer program for calculating time-dependent phenomena involving one-dimensional hydrodynamics, transport, and detailed chemical kinetics. Lawrence Livermore National Laboratory, Livermore, CA, 1995; Revised Report UCRL-52504.
(29) Ó Conaire, M.; Curran, H. J.; Simmie, J. M.; Pitz, W. J.; Westbrook, C. K. *Int. J. Chem. Kinet.* **2004**, *36*, 603.
(30) Healy, D.; Curran, H. J.; Simmie, J. M.; Kalitan, D. M.; Zinner, C. M.; Barrett, A. B.; Petersen, E. L.; Bourque, G. *Combust. Flame* **2008**, *155*, 441.

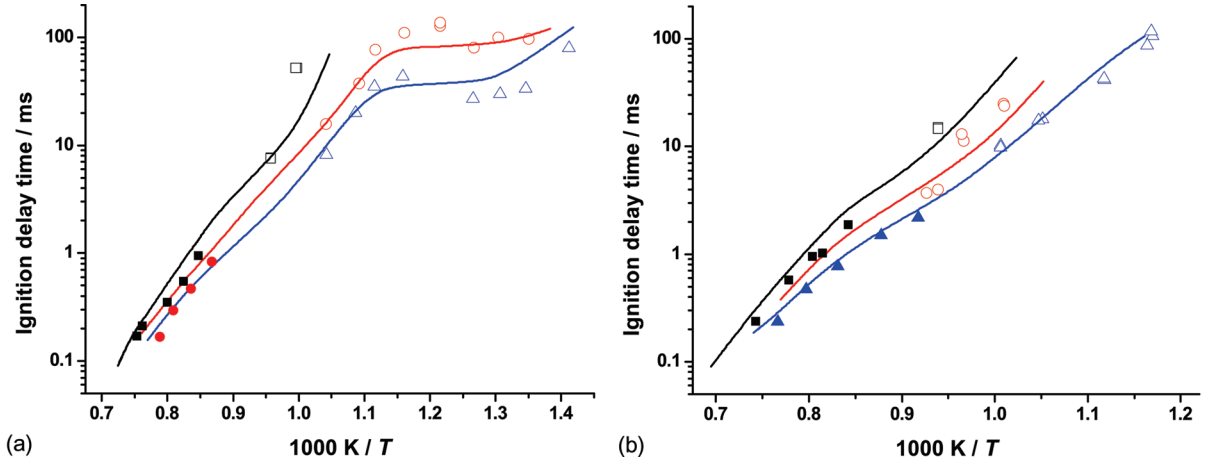

Figure 2. Effect of the pressure on (a) 70/30% $CH_4/n\text{-}C_4H_{10}$ and $\phi = 0.35$ and (b) 90/10% $CH_4/n\text{-}C_4H_{10}$ and $\phi = 0.32$: □, RCM at 10 atm; ■, shock tube at (a) 12 atm and (b) 10 atm; ○, RCM at 20 atm; ●, shock tube at 20 atm; △, RCM at 30 atm; and ▲, shock tube at 33 atm. Lines are model predictions.

simulation was proposed and used by Mittal et al.[31] in simulating their H_2/CO RCM experiments.

HCT treats the RCM as a homogeneous reactor (zone) with a rigid left boundary and a right boundary that can move at any specified velocity (piston velocity). A positive piston velocity is used to simulate compression and/or a decrease in volume, while a negative velocity is used to simulate an expansion process in which the volume increases. Experiments were simulated in three phases: (i) the compression phase from the start of piston motion to the end of compression, (ii) a phase immediately after the end of compression, where the greatest decrease in pressure was observed in each experiment, and (iii) a phase after this to infinite time, with an equally constant but lesser pressure decrease (see Figure 2 of the Supporting Information). When simulating the compression phase, the exact conditions of the experiment are applied. The initial experimental mixture composition, the temperature and pressure, and the experimentally observed/measured compression ratio are used. The constant-volume phases ii and iii were simulated as an adiabatic expansion process, with a greater expansion in phase ii compared to phase iii.

The nonreactive experiments were carried out using (i) pure N_2 diluent, (ii) 80% Ar/20% N_2 diluent, and (iii) 50% Ar/50% N_2 diluent. It was found that the different input parameters to HCT had to be employed in the simulation depending upon the diluent composition used and the initial conditions of pressure and temperature. A comprehensive comparison of simulations versus experimental measurements of nonreactive mixtures was undertaken to successfully simulate the pressure profiles of nonreactive mixtures (see the Supporting Information). Thereafter, the data from these simulations were used in the simulation of the reactive mixtures. Although this simulation is physically unrealistic, this treatment allows for heat losses using a zero-dimensional simulation and a more realistic simulation of the experimental conditions within the RCM.

When the shock-tube experiments were simulated, the region behind the reflected shock wave was assumed to be under constant volume and constant internal energy constraints. For the undiluted fuel−air experiments herein, this assumption is common because it takes into account any pressure rise as a result of the energy release from the reaction process and what subsequent effect it might have on the ignition delay time. As seen in Figure 1, there was no observable pressure rise prior to the main ignition event that would warrant any different assumptions and/or the inclusion of the detailed pressure history of each shock-tube experiment.

4.2. Effect of the Pressure. Both 70/30% and 90/10% blends were studied at varying equivalence ratios, $\phi \approx 0.3$, 0.5, 1.0, and 2.0, and at varying pressures, 10, 16, 20, 26, and 30 atm. Panel a of Figures 2−5 shows the effect of pressure on the 70/30% blend at all four equivalence ratios. It is clear that the ignition limit (being the lowest temperature at which ignition is observed) of the blends increases with a decreasing pressure, from approximately 700 K for both 20 and 30 atm to 950 K for 10 atm at lower equivalence ratios. Whereas this trend is still observed at stoichiometric conditions, the increased reactivity of the fuel results in a narrowing of the gap between the ignition limits at different pressures, until at rich conditions the limits for all three pressures occur between 685 and 695 K.

The 90/10% blend shows similar trends, in panel b of Figures 2−5, more apparently than for the 70/30% blend. The ignition limits also increase with a decreasing pressure; in Figure 2, panel b for example, an ignition limit of 1050 K is observed at a pressure of 10 atm, while at 20 atm this reduces to approximately 950 K and at 30 atm the limit becomes 830 K.

The negative temperature dependence or NTC character of the blends increases with a decreasing pressure. When the ratio of reactivity at the turnover points is compared, i.e., the temperatures at which the region of negative temperature dependence comes to an end, a positive temperature dependence is restored. The simulation predicts that, for all four equivalence ratios of the 70/30% blend, reactivity at this point is decreased by approximately a factor of 3 upon going from 30 to 20 atm and by a factor of approximately 5 upon further decreasing the pressure from 20 to 10 atm. Although only a limited comparison can be made with respect to the 90/10% blend, the decrease in reactivity at the turnover of the NTC region between 30 and 20 atm is of the order of a factor of 2−3, showing similar trends compared to the 70/30% blend. The 90/10% blend contains less butane and is therefore less reactive than the 70/30% blend, resulting in

(31) Mittal, G.; Sung, C. J.; Fairweather, M.; Tomlin, A. S.; Griffiths, J. F.; Hughes, K. J. *Proc. Combust. Inst.* **2007**, *31*, 419.

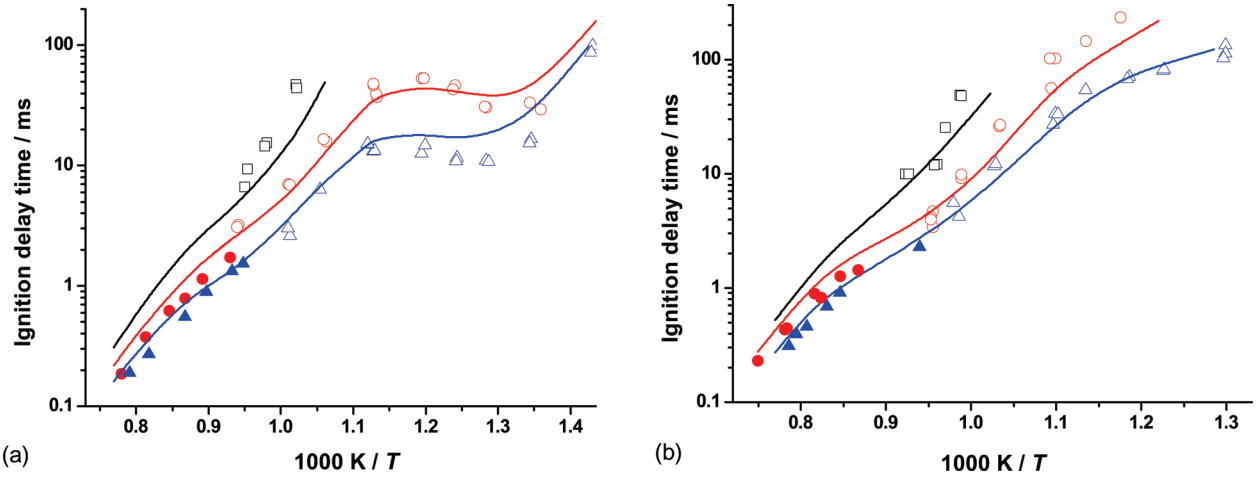

Figure 3. Effect of the pressure on (a) 70/30% $CH_4/n\text{-}C_4H_{10}$ and $\phi = 0.58$ and (b) 90/10% $CH_4/n\text{-}C_4H_{10}$ and $\phi = 0.53$: □, RCM at 10 atm; ○, RCM at 20 atm; ●, shock tube at $\phi = 0.5$ and 16 atm; △, RCM at 30 atm; and ▲, shock tube at $\phi = 0.5$ and 26 atm. Lines are model predictions.

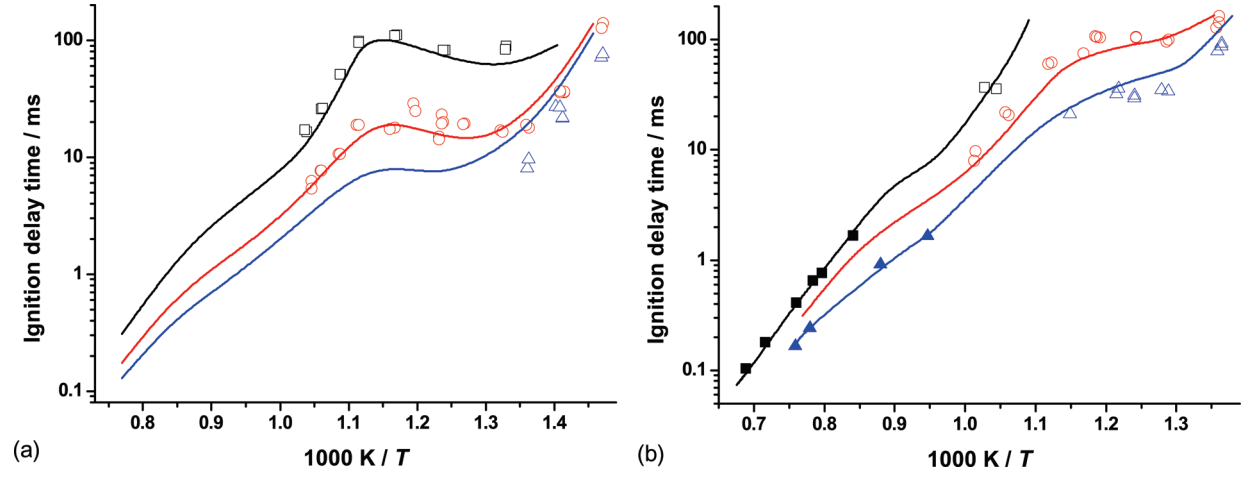

Figure 4. Effect of the pressure on (a) 70/30% $CH_4/n\text{-}C_4H_{10}$ and $\phi = 1.16$ and (b) 90/10% $CH_4/n\text{-}C_4H_{10}$ and $\phi = 1.07$: □, RCM at 10 atm; ■, shock tube at 10 atm; ○, RCM at 20 atm; △, RCM at 30 atm; and ▲, shock tube at 30 atm. Lines are model predictions.

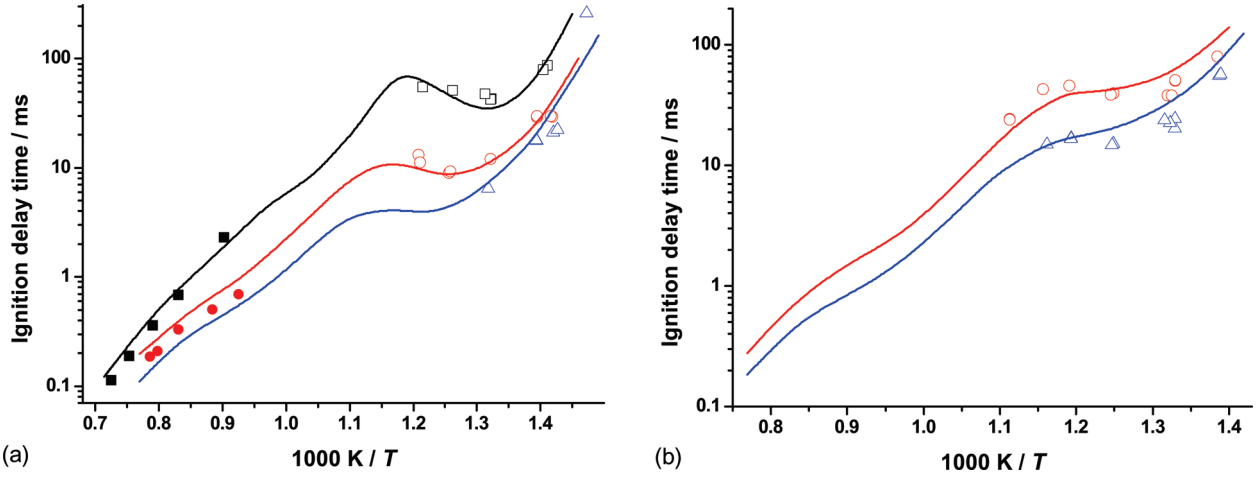

Figure 5. Effect of the pressure on (a) 70/30% $CH_4/n\text{-}C_4H_{10}$ and $\phi = 2.31$ and (b) 90/10% $CH_4/n\text{-}C_4H_{10}$ and $\phi = 2.13$: □, RCM at 10 atm; ■, shock tube at 10 atm; ○, RCM at 20 atm; ●, shock tube at 22 atm; and △, RCM at 30 atm. Lines are model predictions.

higher ignition limits at all pressures. For $\phi = 0.32$ and 0.53, this ignition temperature also lies above the end of the NTC region, making comparisons at the turnover point difficult.

As expected at higher temperatures, the order of reactivity remains the same as at low and intermediate temperatures, with reactivity being greater at higher pressures. In certain cases, such as 90/10% and $\phi = 1.07$, there appears to be a

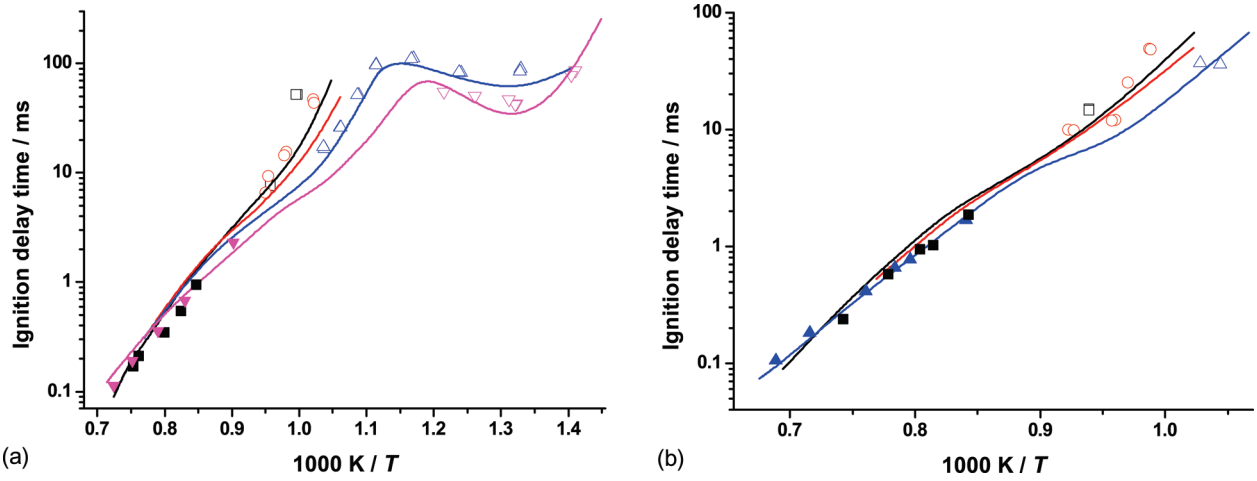

Figure 6. Effect of the equivalence ratio at 10 atm for (a) 70/30% $CH_4/n\text{-}C_4H_{10}$: □, RCM at $\phi = 0.35$; ■, shock tube at $\phi = 0.35$ and 12 atm; ○, RCM at $\phi = 0.58$; △, RCM at $\phi = 1.16$; ▽, RCM at $\phi = 2.31$; and ▼, shock tube at $\phi = 2.31$ and (b) 90/10% $CH_4/n\text{-}C_4H_{10}$: □, RCM at $\phi = 0.32$; ■, shock tube at $\phi = 0.32$; ○, RCM at $\phi = 0.53$; △, RCM at $\phi = 1.07$; and ▲, shock tube at $\phi = 1.07$. Lines are model predictions.

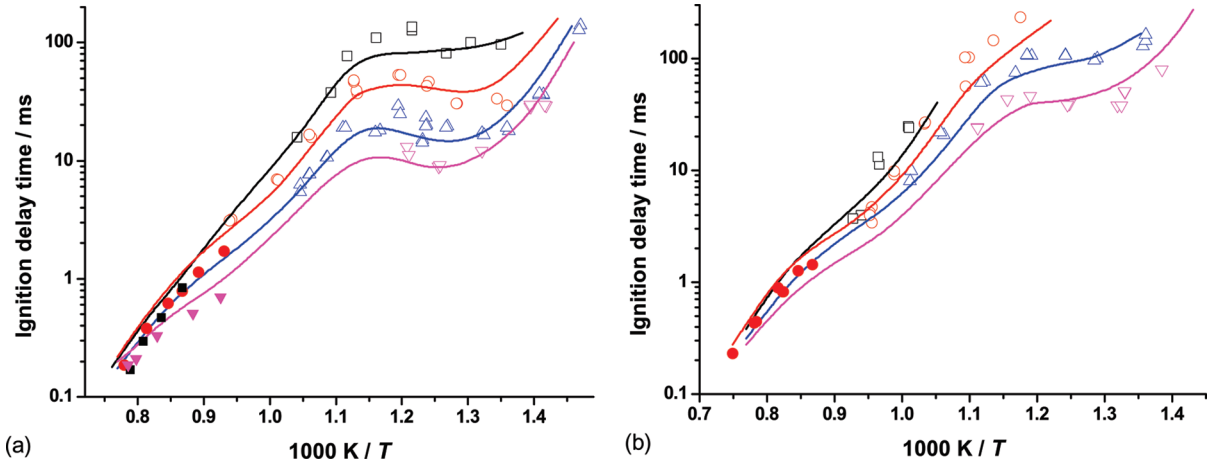

Figure 7. Effect of the equivalence ratio at 20 atm for (a) 70/30% $CH_4/n\text{-}C_4H_{10}$: □, RCM at $\phi = 0.35$; ■, shock tube at $\phi = 0.35$ and 23 atm; ○, RCM at $\phi = 0.58$; ●, shock tube at $\phi = 0.5$ and 26 atm; △, RCM at $\phi = 1.16$; ▽, RCM at $\phi = 2.31$; and ▼, shock tube at $\phi = 2.31$ and 22 atm and (b) 90/10% $CH_4/n\text{-}C_4H_{10}$: □, RCM at $\phi = 0.32$; ○, RCM at $\phi = 0.53$; ●, shock tube at $\phi = 0.5$ and 16 atm; △, RCM at $\phi = 1.07$; and ▽, RCM at $\phi = 2.13$. Lines are model predictions.

divergence between the 10 and 33 atm experiments. This can be explained by examining the conditions of the experiment. Because the reflected-shock pressure or P_5 of all shock-tube experiments dropped slightly as the temperature was increased, the magnitude of this pressure drop varied for each condition, resulting in the observed trends. Each individual shock-tube experiment was simulated using the model and predictions; the results, particularly for the 90/10% blend, are excellent. The model, although predicting the reactivity of the 70/30% blend with slightly lesser accuracy, does reproduce the overall trends at high temperature very well.

4.3. Effect of the Equivalence Ratio. When the pressure is held constant and the equivalence ratio is varied, both the experiment and simulation show the same trends in ignition limits, fuel-rich mixtures having lower ignition limits than fuel-lean mixtures (Figures 6−8). The highest limits are for lean mixtures at lower pressures, which as stated earlier are the conditions at which the most heat loss occurs. For both fuel compositions, the NTC region occurs over the 770−900 K temperature range for each equivalence ratio. This result is not surprising because the NTC chemistry of pure butane has already been observed in this region. At rich conditions, there is a clear trough of reactivity at the onset of the NTC region for both experiment and simulation. This trough is a typical phenomenon associated with NTC behavior, and although it is also present at leaner conditions for the current blends, it is not as pronounced. Thus, the NTC character of the fuel is amplified by increasing the fuel fraction.

Upon moving to higher temperatures, the order of reactivity begins to invert for most cases at approximately 1250 K at lower pressures. This behavior has been reported previously by the authors for both butane isomers.[1,2] At lower temperatures, rich conditions are more reactive, while at temperatures above 1250 K, lean conditions are becoming more reactive. This crossover is reproduced in the simulations of the shock-tube experiments.

4.4. Effect of the Composition. Figures 9−11 illustrate the effect of the composition on the ignition delay time. Because pure methane was studied experimentally herein but is otherwise considered well-known, simulated ignition delay times only for this fuel under these conditions of pressure, temperature, and mixture composition are included. In this way, the relative reactivities of pure methane, 90/10% and

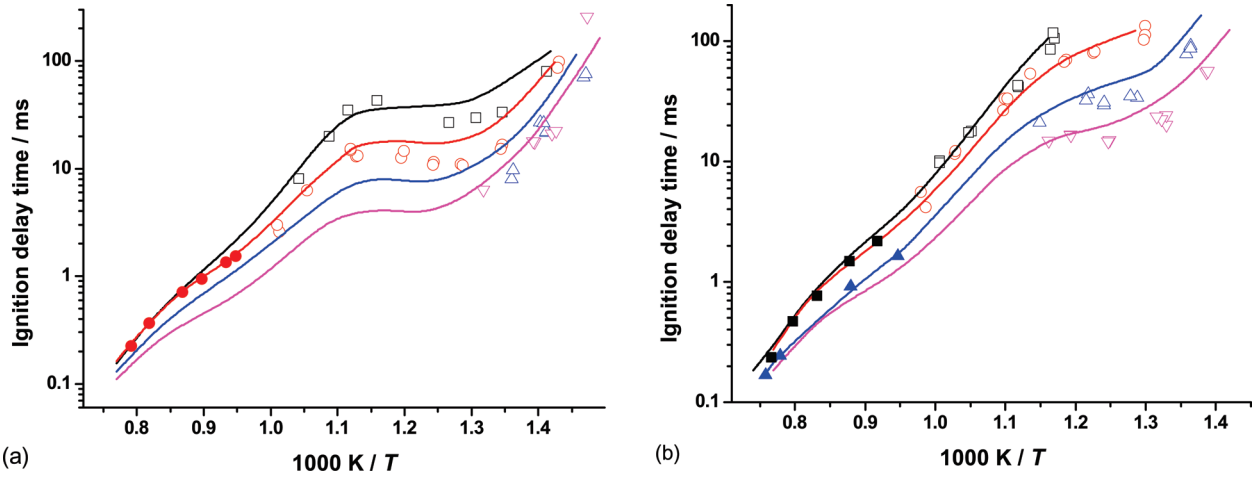

Figure 8. Effect of the equivalence ratio at 30 atm for (a) 70/30% $CH_4/n\text{-}C_4H_{10}$: □, RCM at $\phi = 0.35$; ○, RCM at $\phi = 0.58$; ●, shock tube at $\phi = 0.5$ and 26 atm; △, RCM at $\phi = 1.16$; and ▽, RCM at $\phi = 2.31$ and (b) 90/10% $CH_4/n\text{-}C_4H_{10}$: □, RCM at $\phi = 0.32$; ■, shock tube at $\phi = 0.32$ and 33 atm; ○, RCM at $\phi = 0.53$; △, RCM at $\phi = 1.07$; ▲, shock tube at $\phi = 1.07$; and ▽, RCM at $\phi = 2.13$. Lines are model predictions.

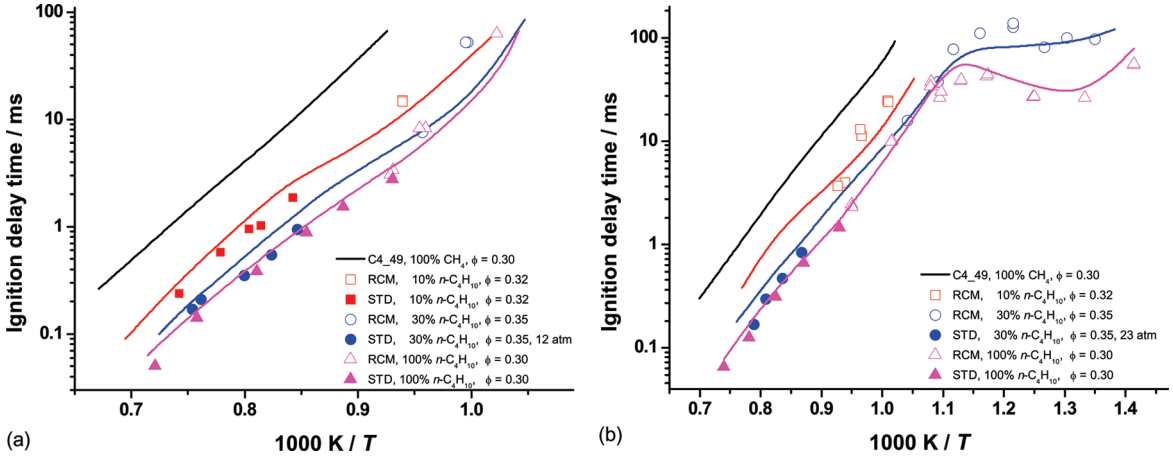

Figure 9. Relative reactivity of methane/*n*-butane mixtures at $\phi \approx 0.3$ and (a) 10 atm and (b) 20 atm. Lines are model simulations, and the 100% *n*-butane data are from Healy et al.[1]

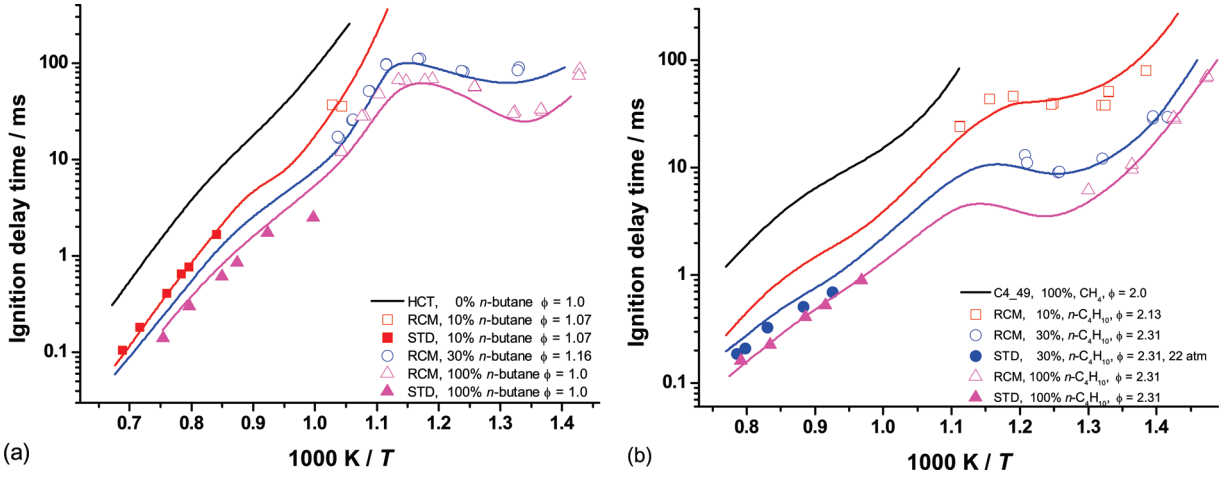

Figure 10. Relative reactivity of methane/*n*-butane mixtures at $\phi \approx 0.5$ and (a) 10 atm and (b) 20 atm. Lines are model simulations, and the 100% *n*-butane data are from Healy et al.[1]

70/30% mixtures of methane/*n*-butane, and pure *n*-butane are compared, with the 100% *n*-butane data coming from the recent work of Healy et al.[1] As expected, in all cases, the pure methane fuel is slowest to ignite, while ignition times decrease with an increasing *n*-butane fraction, with pure *n*-butane mixtures showing the fastest reactivity.

Under lean conditions and at 10 and 20 atm, panels a and b of Figure 9, respectively, the 90% CH_4/10% *n*-C_4H_{10}

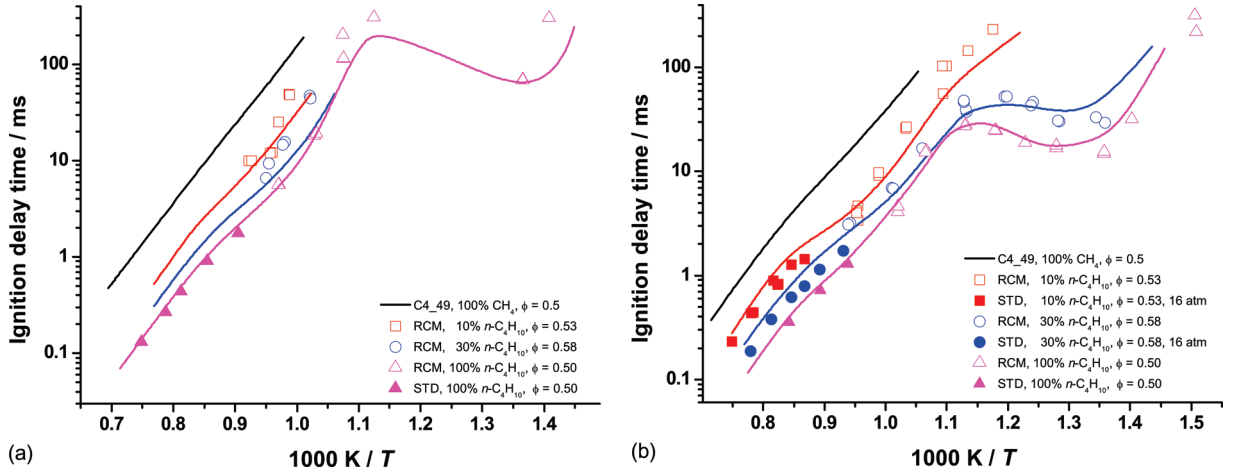

Figure 11. Relative reactivity of methane/*n*-butane mixtures at (a) $\phi \approx 1.0$ and 10 atm and (b) $\phi \approx 2.0$ and 20 atm. Lines are model simulations, and the 100% *n*-butane data are from Healy et al.[1]

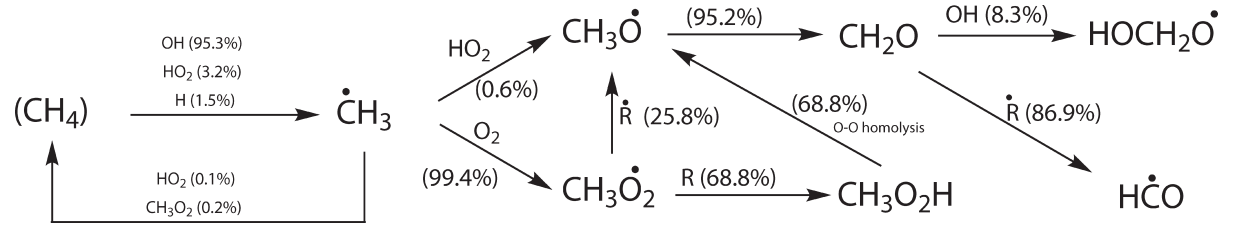

Figure 12. Reaction path analysis for methane fuel: $\phi = 1$, 890 K, 20 bar, and 20% consumption.

mixture ignition delay times are approximately 5 times shorter across the entire temperature range compared to the pure methane simulated times. Ignition delay times for the 70% CH_4/30% *n*-C_4H_{10} mixture are a further 2 times faster compared to the 90/10% mixture, and the associated low-temperature chemistry in the NTC region observed for *n*-butane begins to exhibit itself below 950 K at high pressures. Finally, ignition delay times for pure *n*-butane are observed to be 25% faster than for the 70/30% mixture, and the NTC behavior of *n*-butane is similar to that for the 70/30% blend.

Similar trends are observed at higher equivalence ratios and at varying pressures across the range studied (Figures 10 and 11), in that methane mixtures are slowest to ignite. The 90/10% mixture, although slower in reactivity compared to pure *n*-butane, shows the NTC behavior of butane and an increase in reactivity. This observation is consistent with that first reported by Higgin and Williams when they investigated shock-tube ignition delay time measurements of methane/*n*-butane blends.[4]

For all conditions studied, the lowest temperature at which ignition is observed reduces with an increasing *n*-butane fraction, as shown in Figures 9−11. Ignition for the 90/10% blend normally occurs above or at the end of the NTC region, exhibited by pure *n*-butane, at high equivalence ratios and pressures. However, the 90/10% blend does begin to exert some NTC chemistry, because the ignition occurs at temperatures below the NTC region for these conditions (Figure 11). The 70/30% blend displays an even stronger NTC behavior than the 90/10% blend; the addition of this further 20% *n*-butane results in reactivity of this blend more closely resembling that of pure *n*-butane than its 90/10% counterpart.

The model, besides accurately capturing the lowest temperatures of ignition for both blends and pure *n*-butane, also correctly reproduces the NTC chemistry and the effects of *n*-butane addition to the pure methane fuel. Under rich conditions, because of the high concentration of fuel, the ignition event was quite violent, leading to ignition pressures in excess of 150 atm, and hence, RCM data were not continued further into the NTC region. However, model simulations were performed throughout the entire temperature range and at temperatures above 1000 K, where shock-tube data exist; there is good agreement between the two at rich conditions (Figure 11b).

4.4.1. Fuel Flux Analysis. Fuel flux analyses on both methane and *n*-butane fuels were performed under RCM conditions (Figures 12 and 13). The analyses were carried out at an equivalence ratio of 1.0, pressure of 20 bar, and temperature of 890 K, which is an "average" experimental condition in the middle of the NTC region. The analyses provide a snapshot of the reaction flux after 20% of each fuel has been consumed. For methane (Figure 12), the scheme shows that the fuel mainly undergoes hydrogen abstraction by the $\dot{O}H$ radical, with smaller contributions from $H\dot{O}_2$ and $\dot{H}$ atom to form methyl radicals. The majority of methyl radicals add to molecular oxygen to produce methylperoxyl radicals. Most of these abstract hydrogen from $H\dot{O}_2$ (51.3%), CH_2O (8.2%), C_4H_{10} (5.6%), and CH_3CHO (3.3%) to form methyl hydrogen peroxide, which subsequently decomposes to form methoxyl and hydroxyl radicals. Approximately 25% of methylperoxyl radicals directly produce methoxyl radicals through the reaction with $\dot{C}H_3$ (13.6%), $CH_3\dot{O}_2$ (2.8%), $\dot{C}_2H_5$ (2.7%), and $\dot{C}_3H_5$-a (2.3%). Methoxyl radicals then lose a hydrogen either through direct reaction with molecular oxygen or elimination of $\dot{H}$ atom, forming formaldehyde, most of which undergoes hydrogen

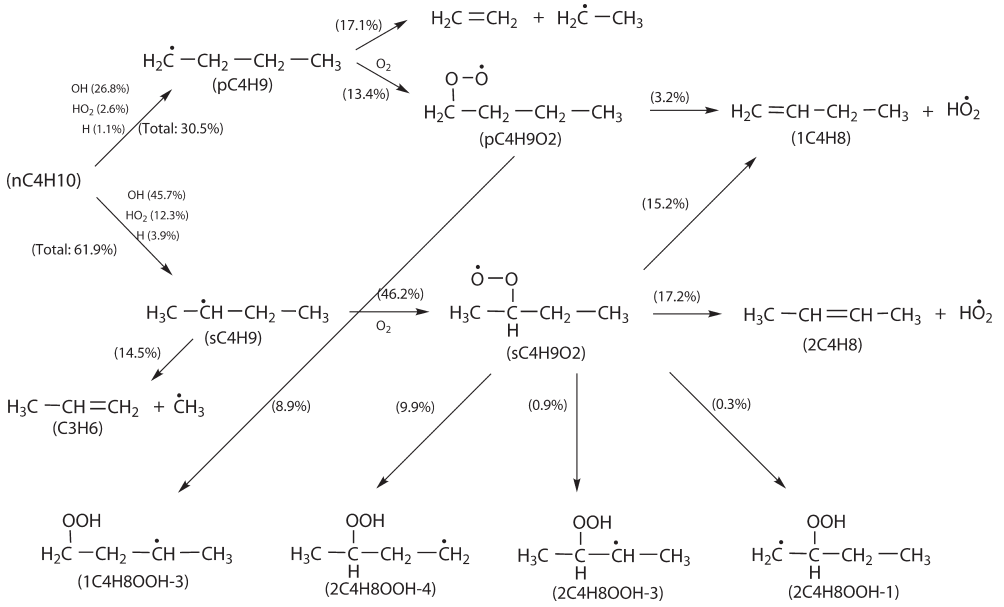

Figure 13. Reaction path analysis for butane fuel: $\phi = 1$, 890 K, 20 bar, and 20% consumption.

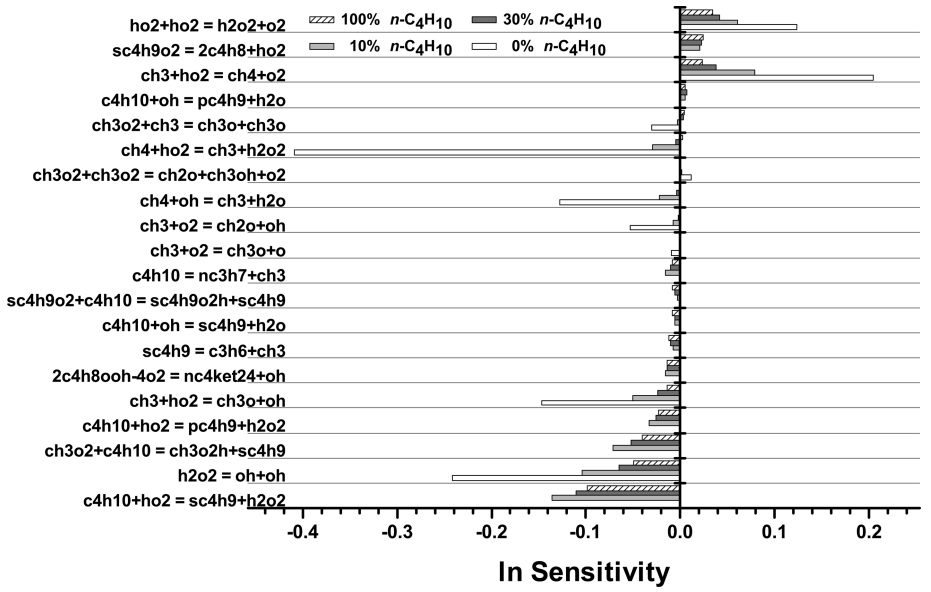

Figure 14. Sensitivity coefficients showing the effect of the composition on the ignition time: $\phi = 1.0$, $p_C = 20$ bar, and 950 K.

abstraction to give formyl radical, with a smaller amount reacting with ȮH to form $HOCH_2\dot{O}$ radical.

The flux analysis for *n*-butane (Figure 13) shows that it undergoes hydrogen abstraction, mainly by ȮH radical, with smaller contributions from $H\dot{O}_2$ and Ḣ, producing *n*-butyl radical, accounting for 30.5% of the total *n*-butane consumption, and *sec*-butyl radical, which accounts for 61.9% of *n*-butane consumption. Just over half of the *n*-butyl radical undergoes β-scission to form ethylene and ethyl radical, with the remainder adding to molecular oxygen, generating *n*-butylperoxy radical. Most of the *sec*-butyl radical adds to molecular oxygen generating the *sec*-butylperoxy species, the *sec*-butyl radical can also undergo β-scission to form propene and a methyl radical, accounting for 14.5% of the overall flux, while the remainder reacts with hydroperoxyl and methylperoxy radicals to produce the *sec*-butoxy radical. The *n*-butylperoxy radical undergoes internal hydrogen atom isomerization to yield *n*-butyl-hydroperoxyl radical, and accounts for 9.8% of the fuel flux. A small amount (0.4%) produces *n*-butyl hydroperoxide by abstracting hydrogen from hydrogen peroxide and *n*-butane. Similarly, *sec*-butyl-peroxy radical produces *sec*-butyl hydroperoxide (1.9%) through reaction with hydrogen peroxide and *n*-butane, while a smaller amount (0.8%) yields *sec*-butoxy radical through reaction with methyl and methyl peroxy radicals with subsequent cleavage of the oxygen-oxygen bond. The *sec*-butyl peroxy radical undergoes internal hydrogen atom isomerization to give *sec*-butyl hydroperoxyl radicals, 11.1% of the total flux, but the vast majority of it proceeds through molecular elimination forming 1-butene (15.2%) and 2-butene (17.2%) and hydroperoxyl radicals. The formation of 1- and 2-butene from butyl-hydroperoxyl radicals are important channels at this temperature because they are the main chain propagation channels in the NTC region, which detract from chain-branching ones, thereby reducing the reactivity of the system.

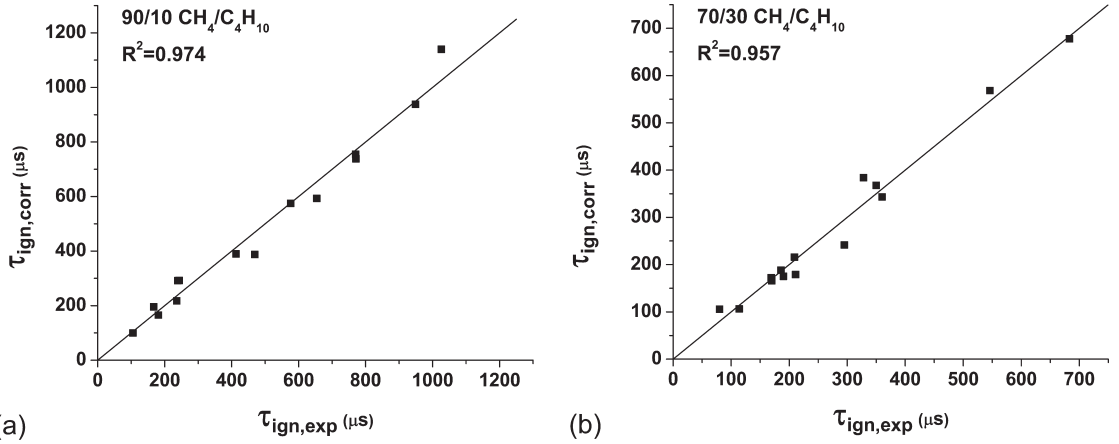

Figure 15. Correlations of high-temperature ignition delay time data (1200−1450 K) for the (a) 90/10% fuel blend and (b) 70/30% fuel blend, with τ_{ign} in microseconds and [fuel] and [air] in mol/cm^3.

4.4.2. Sensitivity Analysis. To amplify this parametric study, a sensitivity analysis was performed to compare the sensitivities of the most important reactions for each composition. The analysis was carried out at stoichiometric conditions, at a pressure of 20 atm and a temperature of 950 K, just above the NTC region. The results of the sensitivity analysis are presented in Figure 14. Reactions with a positive coefficient inhibit reactivity, and those with a negative coefficient promote reactivity. For 100% methane, the most important reaction promoting reactivity is found to be $CH_4 + H\dot{O}_2 = \dot{C}H_3 + H_2O_2$. A product of this reaction, hydrogen peroxide, decomposes to form two hydroxy radicals and is the next most important reaction, H_2O_2 (+M) = $\dot{O}H + \dot{O}H$ (+M). Another important reaction is the reaction of a methyl radical and a hydroperoxyl radical, producing methoxyl and hydroxyl radicals, $\dot{C}H_3 + H\dot{O}_2 = CH_3\dot{O} + \dot{O}H$. This propagation reaction is important because the methoxyl radical can subsequently decompose via β-scission to form formaldehyde and hydrogen atom or can react with molecular oxygen to form formaldehyde and hydroperoxyl radical.

The most important reactions inhibiting reactivity for pure methane at these conditions are $\dot{C}H_3 + H\dot{O}_2 = CH_4 + O_2$ and $H\dot{O}_2 + H\dot{O}_2 = H_2O_2 + O_2$, both of which are termination reactions, which consume hydroperoxyl radicals and, therefore, compete with the most important promoting reaction, which is the reaction of fuel and a hydroperoxyl radical producing a methyl radical and hydrogen peroxide.

When 10% of the methane is replaced with *n*-butane, the sensitivity to these reactions (both positive and negative) is greatly reduced but those that form part of the *n*-butane submechanism become important. The 70/30% methane/*n*-butane blend shows a further reduction in sensitivity to the methane submechanism, but the magnitude of the change is far less compared to that going from pure methane to 90/10% methane/*n*-butane. *n*-Butane chemistry begins to control the reactivity of the 90/10% mixture, with reactions such as $n\text{-}C_4H_{10} + H\dot{O}_2 = s\dot{C}_4H_9 + H_2O_2$ and $n\text{-}C_4H_{10} + CH_3\dot{O}_2 = s\dot{C}_4H_9 + CH_3O_2H$ becoming important. The sensitivities to the *n*-butane submechanism for the 70/30% blend and pure *n*-butane are similar to those seen for the 90/10% mixture, indicating that only a small fraction of *n*-butane will control the reactivity of methane/butane blends.

4.5. High-Temperature Correlations. For each methane/butane split, a high-temperature correlation was developed that predicts ignition delay time as a function of the temperature, pressure, and amount of fuel and air. When plotted on an Arrhenius diagram, the log of the ignition delay time tends to be linear with inverse temperature; thus, the data from the shock-tube experiment lend themselves to such correlations. The correlations herein cover test temperatures from 1200 to 1450 K and follow the equations below for 90/10% and 70/30% methane/butane splits, respectively.

$$\tau_{ign} = 7.33 \times 10^{-9}[\text{fuel}]^{-0.02}[\text{air}]^{-0.60} \exp(40.8/RT)$$

$$\tau_{ign} = 2.23 \times 10^{-9}[\text{fuel}]^{-0.05}[\text{air}]^{-0.84} \exp(40.3/RT)$$

In the preceding equations, τ_{ign} is in microseconds, "fuel" is the concentration of CH_4 plus C_4H_{10} in mol/cm^3, "air" is the concentration of O_2 in mol/cm^3, R is the ideal gas constant in kcal mol^{-1} K^{-1}, and T is the temperature in kelvin. The good agreement between the experimental data and each correlation is shown in Figure 15. Note that the activation energies for both blends are similar, 40.8 and 40.3 kcal/mol. These values can be compared to the ignition activation energy for pure *n*-butane from Healy et al.[1] over a similar range of temperatures and concentrations, which was 40.3 kcal/mol. At the high temperatures of the shock-tube experiments, the effective activation energy from 10% all of the way to 100% C_4H_{10} in air is about the same. Comparisons can also be made to 100% methane. From the earlier study of Petersen et al.,[32] for lean mixtures of methane in air over temperature and pressure ranges of 1370−1660 K and 1−20 atm, the ignition activation energy ranged from about 40 to 44 kcal/mol. In the work by Lamnaouer et al.,[33] a comprehensive methane−air ignition delay time correlation resulted in an overall activation energy of 40.2 kcal/mol. Hence, one can argue that, for temperatures greater than about 1200 K, the ignition activation energies of methane, *n*-butane, and blends of the two in air seem to have values around 40 kcal/mol, independent of the level of methane in the fuel blend.

4.6. Comparison to Methane−Propane Data. The authors have previously published ignition delay time data and simulations using an earlier version of the current model

(32) Petersen, E. L.; Hall, J. M.; Smith, S. D.; de Vries, J.; Amadio, A. R.; Crofton, M. W. *J. Eng. Gas Turbines Power* **2007**, *129*, 937.
(33) Lamnaouer, M.; Ryder, R. C.; Brankovic, A.; Petersen, E. L. *J. Nat. Gas Chem.* **2009**, *18*, 145.

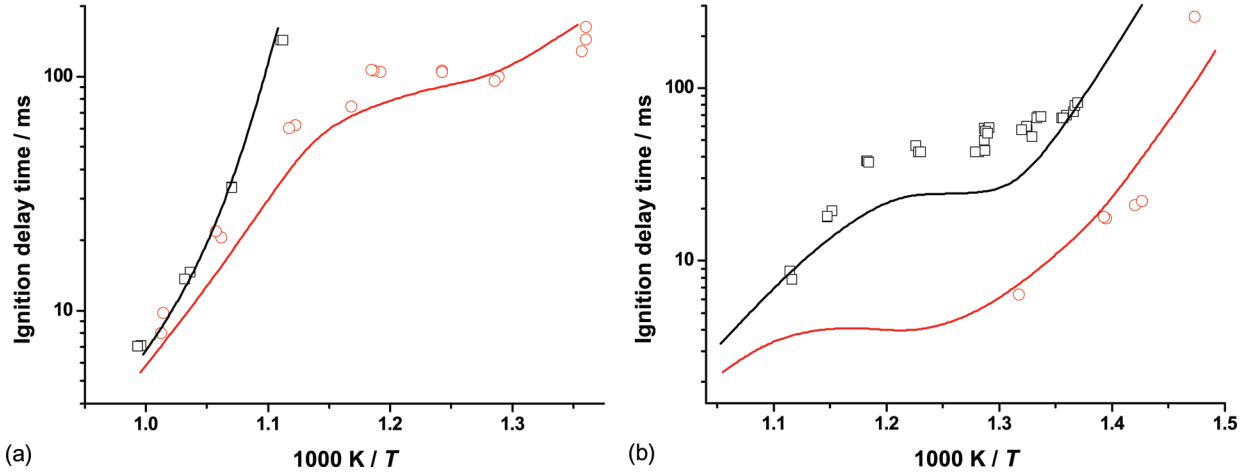

Figure 16. Comparison to CH_4/C_3H_8 ignition delay time measurements[18] at (a) 20 atm: □, 90/10% CH_4/C_3H_8 at $\phi = 1.0$; and ○, 90/10% CH_4/*n*-C_4H_{10} and RCM at $\phi = 1.07$ and (b) 30 atm: □, 70/30% CH_4/C_3H_8 at $\phi = 2.0$; and ○, 70/30% CH_4/*n*-C_4H_{10} at $\phi = 2.31$. Lines are model predictions.

for a similar study of methane/propane blends.[18] Figure 16 shows good agreement between experimental results and model predictions for similar conditions from both studies. Conditions of overlap of both studies are few because of either the methane/propane not reacting at the same conditions as the methane/*n*-butane blends or the methane/*n*-butane blends being so reactive that ignition pressure is too extreme to study at the same conditions as the methane/propane blends.

Figure 16a contrasts the reactivity of each fuel at 20 atm and a fuel ratio of 90/10% close to stoichiometric conditions. Here, the methane/propane mixture is the least reactive, so much that ignition only occurs at temperatures above where NTC chemistry would normally exert itself for this fuel, 910 K. Whereas ignition for the methane/*n*-butane fuel is observed from 740 K upward. At rich conditions and high pressure, the ignition delays and simulation of both fuels can be contrasted from approximately 710 K to the NTC region (Figure 16b). Here, the model is faster than the experiment for high pressure and fuel-rich methane/propane mixtures, but both model and experiment observe similar trends over the entire low-temperature region. Simulations and experiment show a factor-of-three difference between ignition delay times at temperatures below the NTC region for both fuels. The model also predicts a factor-of-eight difference in reactivity during the NTC region as well as reproducing the same behavior as seen experimentally during and after the turnover point of NTC chemistry for the methane/propane fuel (Figure 16b), as it also does for the methane/*n*-butane fuel (Figure 16a).

5. Conclusions

This paper presents a broad range of experimental ignition delay time data for methane/*n*-butane mixtures at temperatures between 660 and 1330 K, pressures of 10, 16, 20, 25, and 30 atm, fuel ratios of 90% CH_4/10% *n*-C_4H_{10} and 70% CH_4/30% *n*-C_4H_{10}, and varying equivalence ratios. Both the experiment and model show that the system is particularly sensitive to the concentration of *n*-butane in the blend, so much that replacing only 30% methane with *n*-butane results in a fuel blend with reactivity more in common with pure *n*-butane than pure methane. Simulations using a chemical kinetic model developed by the authors were found to be in very good agreement with experimental data from both RCM and shock-tube facilities.

Acknowledgment. This work was supported primarily by Rolls-Royce Canada Ltd. Partial support for the experiments came from the National Science Foundation, Grant CBET-0832561, and the Aerospace Corporation. The Texas A&M University (TAMU) authors thank Nicole Donato for help with the experiments and Stefanie Simmons for help with the initial set of fuel-lean shock-tube data.

Supporting Information Available: Supplementary Tables 1−24 and Figures 1−7. This material is available free of charge via the Internet at http://pubs.acs.org.